Maximum Likelihood Receivers for DAPSK Signaling

Lei Xiao, Xiaodai Dong, and Tjeng T. Tjhung

Abstract: **This paper considers the maximum likelihood (ML) detection of 16-ary differential amplitude and phase shift keying (DAPSK) in Rayleigh fading channels. Based on the conditional likelihood function, two new receiver structures, namely ML symbol-by-symbol receiver and ML sequence receiver, are proposed. For the symbol-by-symbol detection, the conventional DAPSK detector is shown to be sub-optimum due to the complete separation in the phase and amplitude detection, but it results in very close performance to the ML detector provided that its circular amplitude decision thresholds are optimized. For the sequence detection, a simple Viterbi algorithm with only two states are adopted to provide an SNR gain around 1 dB on the amplitude bit detection compared with the conventional detector.**

Index Terms: **Differential amplitude and phase shifty keying (DAPSK), maximum likelihood (ML) sequence detection, ML symbol-by-symbol detection, performance analysis, Rayleigh fading channels.**

I. INTRODUCTION

Reliable channel state information (CSI) is often challenging to acquire for wireless coherent receivers. Differential detection circumvents the need for channel estimation by mapping information bits into the phase difference and/or amplitude change of two consecutive symbols. The 16 differential amplitude and phase shift keying (DAPSK), also known as differential 16 star-quadrature amplitude modulation (QAM), encodes three bits into 8 possible phases and one bit into amplitude changes. In the past, detection of the phase bits relied only on the phase difference of two consecutive received symbols and detection of the amplitude bit used only the amplitude information of the received signals [1]–[8]. Hence, the phase decision boundaries are the same as those of 8-DPSK while the amplitude decision boundaries are two circular rings with certain radius as thresholds. *Ad hoc* methods of determining the amplitude detection thresholds include the geometric mean threshold (GMT) approach used in [6] and the arithmetic mean threshold (AMT) scheme proposed in [8]. In [1], Chow *et al.* numerically optimized the differential amplitude detection thresholds, and showed that the bit error rate (BER) performance of 16-DAPSK is approximately 1 dB better than that of 16-differential phase shift keying (DPSK). Optimum amplitude thresholds have

also been evaluated in [4] and [7] for postdetection diversity systems. Whether the separation between the detection of the phase bits and the amplitude bit is optimum or not and how its performance is compared with the maximum likelihood (ML) detector were unknown. In this paper, we develop two optimum ML receiver structures, one for symbol-by-symbol detection and one for ML sequence detection. We show that the conventional 16-DAPSK receiver studied in the literature is only sub-optimum for symbol-by-symbol detection. However, the decision thresholds given in [1] are very good approximations to the maximum likelihood based decision boundaries and negligible signal-to-noise ratio (SNR) loss results from the suboptimum structure. It is further found that if the detector is allowed to have certain memory, i.e., if the symbol-by-symbol condition is removed, then the optimum receiver structure is a maximum likelihood sequence detector (MLSD), which can be implemented by Viterbi algorithm. With moderate extra computational complexity, the MLSD achieves a BER reduction of about fifty percent on the amplitude bit in high SNR's.

The rest of this paper is organized as follows. In Section II, we describe the system model for the reception of DAPSK signals in Rayleigh fading. The conditional likelihood function for the differential decision statistic is derived in Section III. We further develop the ML symbol-by-symbol detector and the ML sequence detector for 16-DAPSK in Sections IV and V, respectively, and compare their performance with the conventional symbol-by-symbol differential detector optimized in [1]. Finally, some conclusions are drawn in Section VI.

II. SYSTEM MODEL

Denote the differential information encoded into two consecutive symbols, the k-th (current) and the $(k-1)$-th (previous) symbols, as α and the previous transmitted symbol as s. The two adjacent received symbols, z_{k-1} and z_k after the matched filter can then be written as

$$z_{k-1} = g_{k-1}s + n_{k-1} \qquad (1a)$$

$$z_k = g_k s\alpha + n_k \qquad (1b)$$

where fading g_{k-1} and g_k are correlated zero-mean complex Gaussian random variables with variance $2E_s$, and n_{k-1} and n_k are independent zero-mean complex additive white Gaussian noise with variance $2N_0$. E_s is the average received energy per symbol. In each channel use, the 16-DAPSK modulation can transmit four bits, where three bits are mapped into the phase difference of two symbols in a way similar to 8-DPSK and another one bit is represented by having the current symbol either stay in the same amplitude ring as the previous symbol or switch to a different ring. Unlike M-DPSK signaling, the closure of the amplitude of transmitted symbols is not guaranteed naturally. Certain rules have to be adopted to make sure

L. Xiao is with the Department of Electrical Engineering, University of Notre Dame, Notre Dame, Indiana, 46556, USA, email: lxiao@nd.edu.

X. Dong is with the Department of Electrical and Computer Engineering, University of Victoria, British Columbia, V8W 3P6, Canada, email: xdong@ece.uvic.ca.

T. T. Tjhung is with the Institute for Infocomm Research, TeleTech Park, 117674, Singapore, email: tjhungtt@i2r.a-star.edu.sg.

$$p_D(r_d, \theta_d | \bar{\alpha}_i e^{j\theta_l}, A_m e^{j\phi_s}) = \frac{r_d \{\gamma_s^2 A_m^4 \bar{\alpha}_i^2 [1 - J_0^2 (2\pi f_D T)] + \gamma_s A_m^2 (1 + \bar{\alpha}_i^2) + 1\}}{\pi [(\gamma_s A_m^2 + 1) r_d^2 + \gamma_s A_m^2 \bar{\alpha}_i^2 + 1 - 2\gamma_s A_m^2 J_0(2\pi f_D T) r_d \bar{\alpha}_i \cos(\theta_l - \theta_d)]^2}. \tag{6}$$

$$p_D(r_d, \theta_d | \bar{\alpha}_i e^{j\theta_l}, A_m e^{j\phi_s}, f_D T = 0) = \frac{r_d [\gamma_s A_m^2 (1 + \bar{\alpha}_i^2) + 1]}{\pi [(\gamma_s A_m^2 + 1) r_d^2 + \gamma_s A_m^2 \bar{\alpha}_i^2 + 1 - 2\gamma_s A_m^2 r_d \bar{\alpha}_i \cos(\theta_l - \theta_d)]^2}. \tag{7}$$

the current symbol αs is still in the signaling set. With a ring ratio of R, the amplitude of the previous symbol $|s|$ can be $\{A_1 = \frac{1}{\sqrt{1+R^2}}, A_2 = \frac{R}{\sqrt{1+R^2}}\}$ and the amplitude of the differential information $|\alpha|$ could be $\{\bar{\alpha}_1 = \frac{1}{R}, \bar{\alpha}_2 = 1, \bar{\alpha}_3 = R\}$. The constraint for closure is if the amplitude of the previous symbol is A_1, then $|\alpha|$ equal to $\bar{\alpha}_2$ or $\bar{\alpha}_3$ is permitted, while only $\bar{\alpha}_1$ or $\bar{\alpha}_2$ is possible when the amplitude of the previous symbol is A_2. We also assume amplitude bit "1" is mapped to "switch" and bit "0" is mapped to "stay."

III. THE LIKELIHOOD FUNCTION

The differential decision statistic for 16-DAPSK can be written as

$$D = r_d e^{j\theta_d} = \frac{z_k}{z_{k-1}} = \frac{g_k s\alpha + n_k}{g_{k-1}s + n_{k-1}} \triangleq \frac{X}{Y}. \tag{2}$$

Conditioned on the previous symbol $s = A_m e^{j\phi_s}$ and the differential information $\alpha = \bar{\alpha}_i e^{j\theta_l}$, where $m \in \{1, 2\}$, ϕ_s is the phase of the $(k-1)$-th transmitted symbol, $i \in \{1, 2, 3\}$ and $\theta_l = 2\pi l/8, l = 0, \cdots, 7$, D is in the form of the ratio between two correlated complex Gaussian random variables. The conditional probability density function (PDF) can be written as [9, (13)]

$$p_D(r_d, \theta_d | \bar{\alpha}_i e^{j\theta_l}, A_m e^{j\phi_s})$$
$$= \frac{|\mathbf{L}|}{\pi} \frac{r_d}{(m_{yy} r_d^2 + m_{xx} - 2\Re\{m_{xy}^* r_d e^{j\theta_d}\})^2} \tag{3}$$

where m_{xx}, m_{yy}, m_{xy} are the second central moments of X and Y, while $\mathbf{L}$ is the Hermitian covariance matrix as given by [9]

$$\mathbf{L} = \begin{pmatrix} m_{xx} & m_{xy} \\ m_{xy}^* & m_{yy} \end{pmatrix}. \tag{4}$$

The moments, conditioned on $\bar{\alpha}_i e^{j\theta_l}$ and $A_m e^{j\phi_s}$, are

$$m_{xx} = 2E_s A_m^2 \bar{\alpha}_i^2 + 2N_0 \tag{5a}$$
$$m_{yy} = 2E_s A_m^2 + 2N_0 \tag{5b}$$
$$m_{xy} = 2E_s J_0(2\pi f_D T) A_m^2 \bar{\alpha}_i e^{j\theta_l} \tag{5c}$$

where a 2-D isotropic channel correlation model is assumed, f_D is the maximum Doppler frequency, T is the symbol interval, and $J_0(\cdot)$ is the zeroth order Bessel of the first kind. Substituting (4) and (5) into (3), the conditional PDF of D can be expressed as in (6) shown at the top of the page. We use γ_s to denote the average SNR per symbol, which is defined as E_s/N_0. If the channel remains constant over the consecutive two channel use, i.e., $f_D T = 0$, the conditional PDF can be simplified as in (7) given at the top of the page. Note that the PDF (6) is independent of the phase of the previous transmitted symbol ϕ_s, and therefore ϕ_s can be dropped from the left-hand side of (6).

IV. THE ML SYMBOL-BY-SYMBOL DETECTOR

From the conditional PDF in (6), the decision rule for ML symbol-by-symbol detection is to find the phase $\theta_l \in \{2\pi l/8: l = 0, \cdots, 7\}$ and the amplitude bit in $\{0, 1\}$ that maximize the likelihood function

$$\{p_D(r_d, \theta_d | \bar{\alpha}_2 e^{j\theta_l}, A_1) + p_D(r_d, \theta_d | \bar{\alpha}_2 e^{j\theta_l}, A_2)$$
$$\text{or } p_D(r_d, \theta_d | \bar{\alpha}_1 e^{j\theta_l}, A_2) + p_D(r_d, \theta_d | \bar{\alpha}_3 e^{j\theta_l}, A_1)\}. \tag{8}$$

It is seen from (6) and (8) that a "minimum distance" decision rule is optimum for the differential angular information, since the term inside the square of the denominator of (6) is positive definite thus maximizing $\cos(\theta_l - \theta_d)$ is needed to minimize the denominator of the conditional likelihood function, which does not depend on the envelope information. That is,

$$\hat{\theta} = \arg \max_{\theta_l} \{\cos(\theta_l - \theta_d)\}. \tag{9}$$

And then the likelihood function for the amplitude bit is written as

$$L(0) = p_D(r_d, \theta_d | \bar{\alpha}_2 e^{j\hat{\theta}}, A_1) + p_D(r_d, \theta_d | \bar{\alpha}_2 e^{j\hat{\theta}}, A_2) \tag{10a}$$
$$L(1) = p_D(r_d, \theta_d | \bar{\alpha}_1 e^{j\hat{\theta}}, A_2) + p_D(r_d, \theta_d | \bar{\alpha}_3 e^{j\hat{\theta}}, A_1) \tag{10b}$$

where the ML symbol-by-symbol detection of differential amplitude information requires the phase error information $\cos(\hat{\theta} - \theta_d)$. $L(0)$ is the likelihood of "0" being the amplitude bit, while $L(1)$ is that of "1" being the amplitude bit. We define a new function as

$$K(r_d, \theta_d, \hat{\theta}) = L(0) - L(1) \tag{11}$$

and the ML symbol-by-symbol receiver can be constructed from (11) and (9) as shown in Fig. 1. It is worth noting $K(r_d, \theta_d, \hat{\theta})$ is also a function of the normalized Doppler frequency and the average SNR, as indicated by (6). In practice, either the estimation of these values [10] or an experimental typical value can be used for these parameters in calculating the likelihood function. The conventional receiver [1]–[3], [5] does not utilize the phase error information $\cos(\hat{\theta} - \theta_d)$, while the optimum receiver incorporates an ML phase detector in the decision of the amplitude bit.

The optimum phase decision boundaries are the same as those of 8-PSK. The optimum amplitude decision boundaries can be determined by solving $K(r_d, \theta_d, \hat{\theta}) = 0$ numerically for r_d given a $\theta_d \in \{0, 2\pi\}$ and $\hat{\theta}$ obtained from (9). Two roots exist for this equation and they correspond to a point on the upper amplitude decision boundary and a point on the lower amplitude decision boundary respectively. An interesting observation from (6), (10), and (11) is that $K(r, \theta_d, \hat{\theta}) = 0 \Leftrightarrow K(1/r, \theta_d, \hat{\theta}) = 0$, which means for every θ_d, the optimum upper and lower amplitude decision boundaries are reciprocal. The 2-D constellation
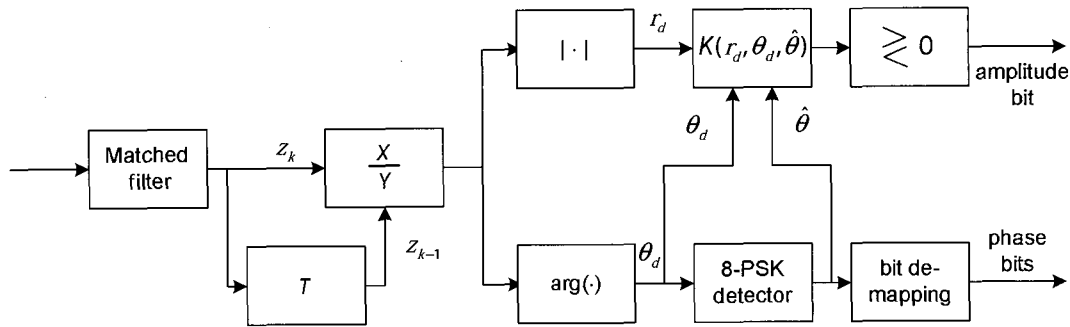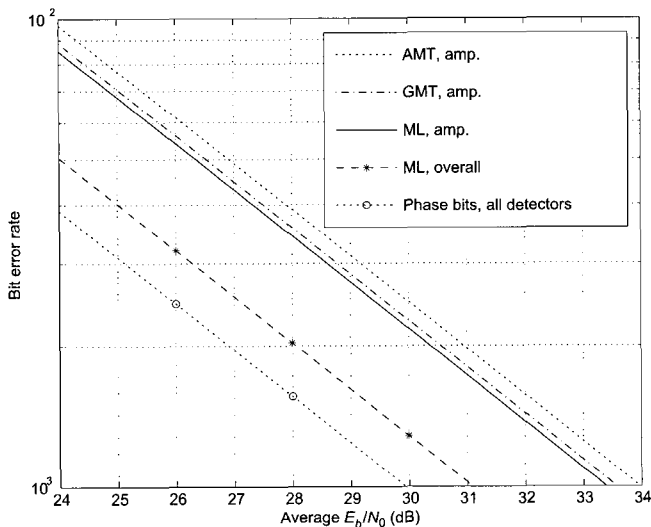
Fig. 1. The ML symbol-by-symbol detector for 16-DAPSK signaling.

Fig. 3.   The error probability of the amplitude bit and phase bits for AMT [8], GMT [6], and the new ML symbol-by-symbol receiver for 16-DAPSK, $f_D T = 0$ is assumed.

of the differential information α in 16-DAPSK with a ring ratio of 2 and its decision boundaries for several SNR levels are plotted in Fig. 2. Signal points on this constellation correspond to possible α values. It is observed that the optimum amplitude decision boundaries are dependent on SNR and approach asymptotic upper and lower boundaries as the SNR gets large. The circular amplitude decision boundaries with optimized radii for high SNR's as presented by [1] are also shown in Fig. 2 and are actually circular approximations to the new asymptotic ML boundaries. The optimum outer decision circle radius was found to be reciprocal to the inner decision circle radius in [1] through numerical search, while our formulation verifies this relationship analytically.

Numerical integration of the likelihood function can be employed to evaluate the amplitude error performance of the new ML symbol-by-symbol receiver once the decision boundaries are determined numerically. The exact BER's of the ML receiver and the conventional receiver are derived in the appendix. The amplitude BER's for the conventional receiver with optimized thresholds [1] and the ML symbol-by-symbol receiver are listed and compared in Table 1. Numerical search has been performed to find the optimum ring ratio that minimizes the error probability of DAPSK signaling with ML symbol-by-symbol

detection. It is found that the optimum ring ratio at 20 dB is $R = 2.02$, which is close to the ring ratio of $R = 2$ optimized by Chow et al. in [1] for the threshold receiver. Hence, the ring ratio of $R = 2$ is adopted for all the results in this paper. The conventional detection in Table 1 refers to the threshold amplitude detector with threshold value optimized in [1], and the 4-DAPSK, 8-DAPSK, and 16-DAPSK are DAPSK constellations with two amplitude levels and 2, 4, and 8 possible phases, respectively. Note that the conventional receiver does not use the phase error information so that its amplitude error probability does not vary with the number of possible phases. The new ML symbol-by-symbol receiver, however, makes use of the phase error information $\cos(\hat{\theta} - \theta_d)$ and therefore has a lower amplitude error probability when there are fewer possible phases in the constellation. As expected from the asymptotic boundaries in Fig. 2, the performance improvement is minimal. In Fig. 3, we compare the performance of our ML symbol-by-symbol detector with the AMT and GMT discussed in [6] and [8]. At the BER level of 10^{-3}, the AMT suffers an SNR loss of 0.48 dB, and the GMT incurs an SNR penalty of 0.17 dB, both relative to the ML symbol-by-symbol detector. This is because the decision thresholds in AMT and GMT are poorly chosen.

V. THE ML SEQUENCE DETECTOR

In the construction of the ML symbol-by-symbol detector in Section IV, we assume no knowledge of the amplitude of the previous symbol s. Averaging over all possible $|s|$'s are necessary to obtain the likelihood function from the conditional likelihood function (6). This inevitably increases the ambiguity of the likelihood function. If, instead, we are able to consider the amplitude of the previous symbol s for the detection of the differential information, there will be a potential gain in performance due to a sharper likelihood function.

The two possible amplitude values of the previous transmitted symbol are the two states in a trellis as shown in Fig. 4. This is a system with memory length 1. It has been shown in [11, Appendix F] that Viterbi algorithm is ML for the sequence detection over a trellis. Similar to the symbol-by-symbol detection case, the "minimum distance" decision rule (9) is maximum likelihood for the differential angular bits. Once the phase decision $\hat{\theta}$ is made from this detection rule, it is fed into the conditional likelihood function given by (6) to calculate the four path metrics $M_{i,j}$, where $i, j \in \{1, 2\}$. Logarithm of the metrics $M_{i,j}$'s are used in our sequence detector in order to transform
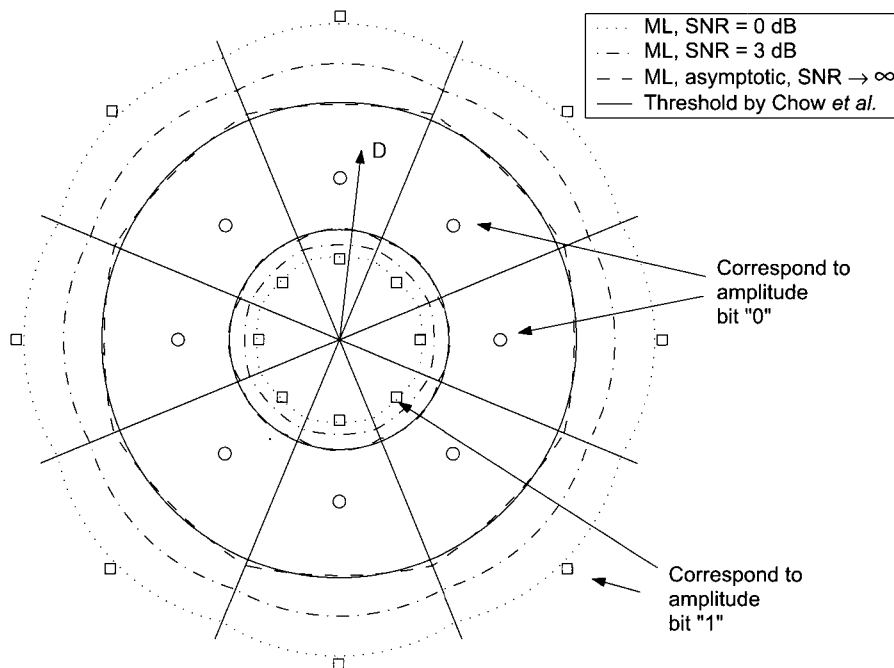
Fig. 2. The ML decision boundaries for differential signal points $\alpha = \bar{\alpha}_i e^{j\theta_i}$ at different SNR's and the decision threshold optimized in [1]. The ring ratio of 16-DAPSK is 2 and $f_D T = 0$.

Table 1. Comparison between Chow's threshold detector [1] and ML symbol-by-symbol detector. The normalized Doppler frequency is $f_D T = 0$.

Amplitude detection for 16-DAPSK			
SNR (dB)	BER, conventional detection [1]	BER, ML symbol-by-symbol	BER reduction
0 dB	4.7307×10^{-1}	4.7056×10^{-1}	0.53%
10 dB	$2.9829e \times 10^{-1}$	2.9790×10^{-1}	0.13%
20 dB	7.1932×10^{-2}	7.1823×10^{-2}	0.15%
30 dB	8.5786×10^{-3}	8.5595×10^{-3}	0.22%
40 dB	8.7527×10^{-4}	8.7325×10^{-4}	0.23%
Amplitude detection for 8-DAPSK			
SNR (dB)	BER, conventional detection [1]	BER, ML symbol-by-symbol	BER reduction
0 dB	4.7307×10^{-1}	4.7021×10^{-1}	0.60%
10 dB	$2.9829e \times 10^{-1}$	2.9752×10^{-1}	0.26%
20 dB	7.1932×10^{-2}	7.1472×10^{-2}	0.64%
30 dB	8.5786×10^{-3}	8.5169×10^{-3}	0.72%
40 dB	8.7527×10^{-4}	8.6893×10^{-4}	0.72%
Amplitude detection for 4-DAPSK			
SNR (dB)	BER, conventional detection [1]	BER, ML symbol-by-symbol	BER reduction
0 dB	4.7307×10^{-1}	4.6929×10^{-1}	0.80%
10 dB	$2.9829e \times 10^{-1}$	2.9675×10^{-1}	0.51%
20 dB	7.1932×10^{-2}	7.1351×10^{-2}	0.81%
30 dB	8.5786×10^{-3}	8.5060×10^{-3}	0.85%
40 dB	8.7527×10^{-4}	8.6781×10^{-4}	0.85%

the multiplicative metrics into the additive decision metrics.

It is observed from (6) that both the average SNR γ_s and the normalized Doppler frequency $f_D T$ (or equivalently, correlation of the channel gains) are required for ML sequence detection. More often than not, accurate estimates of these parameters, especially the Doppler frequency, are not easily available at the receiver. In the rest of this section, we use simulation results to reveal the effect of these parameters on the performance of the

ML sequence detector. The simulation results for the amplitude bit error rates of the conventional and the new MLSD detectors are presented in Figs. 5 and 6 as a function of the average SNR per bit, for a normalized Doppler frequency of $f_D T = 0.003$ and $f_D T = 0.01$, respectively. The correlated Rayleigh fading generator described in [12] is used in our simulation. For systems without average SNR estimations, we fix our guess as 40 dB in calculating the decision metrics, as the BER is about

$$M_{1,1} = p_D(r_d, \theta_d | \tilde{\alpha}_2 e^{j\theta}, A_1) \qquad M_{1,2} = p_D(r_d, \theta_d | \tilde{\alpha}_3 e^{j\theta}, A_1)$$

$$M_{2,1} = p_D(r_d, \theta_d | \tilde{\alpha}_1 e^{j\theta}, A_2) \qquad M_{2,2} = p_D(r_d, \theta_d | \tilde{\alpha}_2 e^{j\theta}, A_2)$$
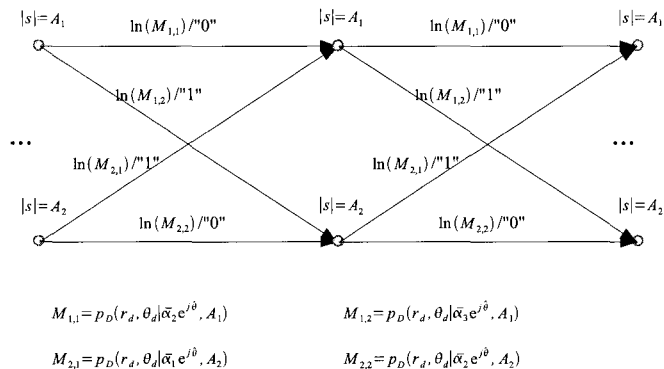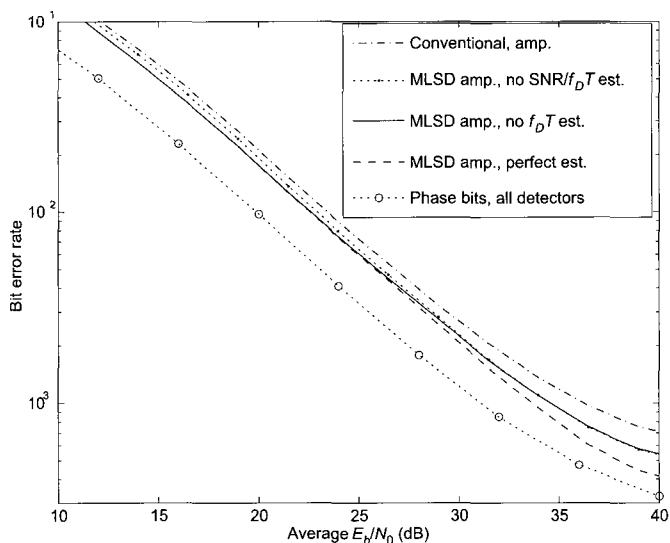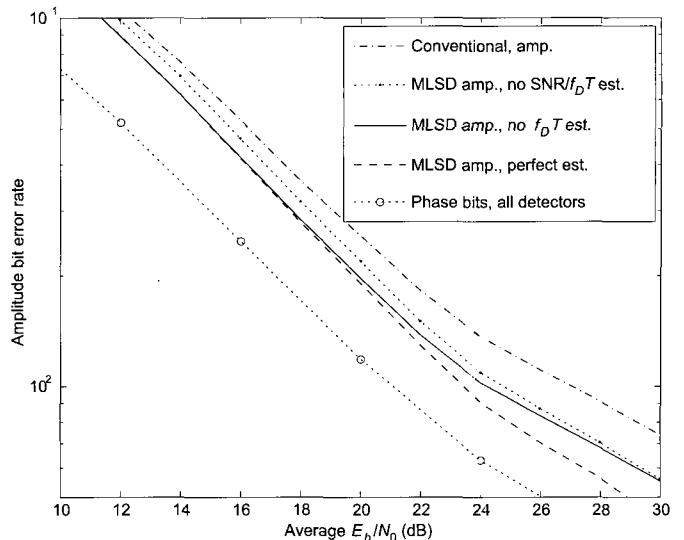
Fig. 4. The trellis for the amplitude bit detection of the DAPSK signals.

Fig. 5. The error probability of the amplitude bit and phase bits for the conventional receiver and the MLSD receivers, assuming different knowledge of the channel. The normalized Doppler frequency is $f_D T = 0.003$.

10^{-3} at 40 dB. For systems without Doppler spread (channel correlation) estimations, we use $f_D T = 0$ for (6) in the metrics calculation. Since the estimation for the Doppler spread is more difficult than that for the average SNR, we assume no Doppler information is available when the average SNR is not known. To further simplify the scenario, we assume the average SNR and Doppler spread estimations are perfect whenever available. From Figs. 5 and 6, it is observed that the gain for using MLSD increases with the increase of the average SNR. In the high SNR region, the MLSD's achieve about 1 dB in SNR savings and about fifty percent error reduction in BER. The MLSD's with or without the Doppler spread estimation perform almost the same before the occurrence of the error floor, while the MLSD without the average SNR information exhibits less gain compared with those with the information of average SNR in this region. In the error-floor region, however, the knowledge of average SNR alone does not seem to provide any gain in performance. Since most of the systems are designed to operate in the error-floor-free region, our simulation results suggest using MLSD with average SNR estimations. Finally, the performance gain of MLSD receivers over the conventional receiver is more

Fig. 6. The error probability of the amplitude bit and phase bits for the conventional receiver and the MLSD receivers, assuming different knowledge of the channel. The normalized Doppler frequency is $f_D T = 0.01$.

pronounced in a channel with higher fading rate.

VI. CONCLUSION

Two maximum likelihood detectors for 16-DAPSK have been synthesized from the probability distribution function of the differential decision statistic. We have shown that although the conventional DAPSK receiver that utilizes the received phase and envelope separately is sub-optimum, it results in negligible performance degradation compared to the optimum symbol-by-symbol detector if its amplitude decision threshold is optimized. The AMT and GMT schemes, however, incur substantial SNR loss due to the ad hoc decision threshold. Moreover, a simple Viterbi algorithm can be used to perform the ML sequence detection. The necessity for estimating different channel parameters, namely the average SNR and the maximum Doppler frequency, have been investigated using simulation. An SNR saving of 1 dB over the conventional differential receiver is observed due to the optimality of the MLSD. The ML design and analysis in this paper can be easily extended to signaling formats with more than two amplitude levels.

APPENDIX

In this appendix, we derive the exact BER of 16-DAPSK signaling in Rayleigh fading channels. There are three bits differentially encoded in the phase and one bit modulated in the amplitude, so the BER of 16-DAPSK is given by

$$P_b(e) = \frac{3}{4} P_{b,p}(e) + \frac{1}{4} P_{b,a}(e) \tag{12}$$

where $P_{b,p}(e)$ and $P_{b,a}(e)$ are the exact BER of the phase bits and the amplitude bit, respectively. Without loss of generality, suppose differential phase $\theta_l = 0$ was transmitted. The BER of the phase bits for the conventional differential detection and

the ML symbol-by-symbol detection are the same, and can be calculated from the transition probabilities as

$$P_{b,p}(e) = \frac{1}{3}\sum_{k=1}^{7} w_k P(\hat{\theta} = 2\pi k/8|\theta_l = 0) \tag{13}$$

where w_k is the Hamming distance between the bit pattern designated to the phase $\frac{2\pi k}{8}$ ($k \neq 0$) and that designated to the zero phase, and $P(\hat{\theta} = 2\pi k/8|\theta_l = 0)$ is the transition probability that $\hat{\theta} = 2\pi k/8$ was decided in error given the zero transmitted differential phase, i.e.,

$$P(\hat{\theta} = 2\pi k/8|\theta_l = 0)$$
$$= \frac{1}{4}\int_{\frac{2k-1}{8}\pi}^{\frac{2k+1}{8}\pi}\int_0^\infty p_D(r_d, \theta_d|\bar{\alpha}_3 e^{j\theta_l}, A_1)\mathrm{d}r_d\mathrm{d}\theta_d$$
$$+ \frac{1}{4}\int_{\frac{2k-1}{8}\pi}^{\frac{2k+1}{8}\pi}\int_0^\infty p_D(r_d, \theta_d|\bar{\alpha}_2 e^{j\theta_l}, A_1)\mathrm{d}r_d\mathrm{d}\theta_d$$
$$+ \frac{1}{4}\int_{\frac{2k-1}{8}\pi}^{\frac{2k+1}{8}\pi}\int_0^\infty p_D(r_d, \theta_d|\bar{\alpha}_1 e^{j\theta_l}, A_2)\mathrm{d}r_d\mathrm{d}\theta_d$$
$$+ \frac{1}{4}\int_{\frac{2k-1}{8}\pi}^{\frac{2k+1}{8}\pi}\int_0^\infty p_D(r_d, \theta_d|\bar{\alpha}_2 e^{j\theta_l}, A_2)\mathrm{d}r_d\mathrm{d}\theta_d \tag{14}$$

where each integral term can be solved as

$$\int_{\frac{2k-1}{8}\pi}^{\frac{2k+1}{8}\pi}\int_0^\infty p_D(r_d, \theta_d|\bar{\alpha}_i e^{j\theta_l}, A_m)\mathrm{d}r_d\mathrm{d}\theta_d$$
$$= \int_{\frac{2k-1}{8}\pi}^{\frac{2k+1}{8}\pi} \frac{\Gamma}{\pi}\left[\frac{2}{\Delta} - \frac{\pi b}{\Delta^{3/2}} + \frac{2b}{\Delta^{3/2}}\tan^{-1}\left(\frac{b}{\sqrt{\Delta}}\right)\right]\mathrm{d}\theta_d \tag{15a}$$

where [9, (19a)] has been used, and

$$\Gamma = \gamma^2 A_m^4\bar{\alpha}_i^2\left[1 - J_0^2(2\pi f_D T)\right]$$
$$\quad + \gamma A_m^2(1 + \bar{\alpha}_i^2) + 1 \tag{15b}$$
$$a = 1 + \gamma A_m^2\bar{\alpha}_i^2 \tag{15c}$$
$$b = -2\gamma A_m^2 J_0(2\pi f_D T)\bar{\alpha}_i\cos\theta_d \tag{15d}$$
$$c = \gamma A_m^2 + 1 \tag{15e}$$
$$\Delta = 4ac - b^2. \tag{15f}$$

We denote the maximum likelihood amplitude decision boundaries which are functions of θ_d as $R_1(\theta_d)$ and $R_2(\theta_d) = \frac{1}{R_1(\theta_d)}$, where $R_1(\theta_d)$ is the smaller positive solution for the equation $K(r_d, \theta_d, \hat{\theta}) = 0$ for a given θ_d and have to be calculated numerically. For the conventional receiver, $R_1(\theta_d)$ and $R_2(\theta_d)$ are reciprocal constants. The bit error probability of the amplitude bit is given by

$$P_{b,a}(e) = \frac{1}{2}P_{b,a}(e|\text{"0"}) + \frac{1}{2}P_{b,a}(e|\text{"1"}) \tag{16a}$$

where $P_{b,a}(e|\text{"0"})$ and $P_{b,a}(e|\text{"1"})$ are the probability of error when the amplitude is "0" or "1," respectively. Invoking symmetry on phase again, we can assume $\theta_l = 0$ was transmitted

and formulate $P_{b,a}(e|\text{"0"})$ as

$$P_{b,a}(e|\text{"0"}) = P_{b,a}(e|\text{"0"}, \theta_l = 0)$$
$$= 1 - \frac{1}{2}\int_0^{2\pi}\int_{R_1(\theta_d)}^{R_2(\theta_d)} p_D(r_d, \theta_d|\bar{\alpha}_2 e^{j\theta_l}, A_1)\mathrm{d}r_d\mathrm{d}\theta_d$$
$$- \frac{1}{2}\int_0^{2\pi}\int_{R_1(\theta_d)}^{R_2(\theta_d)} p_D(r_d, \theta_d|\bar{\alpha}_2 e^{j\theta_l}, A_2)\mathrm{d}r_d\mathrm{d}\theta_d \tag{16b}$$

and $P_{b,a}(e|\text{"1"})$ in the similar form

$$P_{b,a}(e|\text{"1"}) = P_{b,a}(e|\text{"1"}, \theta_l = 0)$$
$$= \frac{1}{2}\int_0^{2\pi}\int_{R_1(\theta_d)}^{R_2(\theta_d)} p_D(r_d, \theta_d|\bar{\alpha}_3 e^{j\theta_l}, A_1)\mathrm{d}r_d\mathrm{d}\theta_d$$
$$+ \frac{1}{2}\int_0^{2\pi}\int_{R_1(\theta_d)}^{R_2(\theta_d)} p_D(r_d, \theta_d|\bar{\alpha}_1 e^{j\theta_l}, A_2)\mathrm{d}r_d\mathrm{d}\theta_d. \tag{16c}$$

Some note on the formulation of (16). The amplitude decision region for bit "0," as depicted in Fig. 2, is the area between $R_2(\theta_d)$ and $R_1(\theta_d)$ for each θ_d. The four integrations in (16), therefore, integrate likelihood functions over the decision region of bit "0." For likelihood functions correspond to bit "0" sent, the result of the integration is the probability of a correct decision and its complementary is the probability of error for this combination of previous signal amplitude and current differential information amplitude; while the integration of the likelihood functions correspond to bit "1" directly yield the error probabilities for the specific previous signal amplitude and current differential information amplitude. Finally, we observe that the two possible combinations of A_m and α_i given the amplitude bit are equally likely, and hence the factor of one-half on each integral.

Using [9, (19a)], each integral term in (16) is solved as

$$\int_0^{2\pi}\int_{R_1(\theta_d)}^{R_2(\theta_d)} p_D(r_d, \theta_d|\bar{\alpha}_i e^{j\theta_l}, A_m)\mathrm{d}r_d\mathrm{d}\theta_d$$
$$= \int_0^{2\pi}\frac{\Gamma}{\pi}\left[\frac{2b}{\Delta^{3/2}}\tan^{-1}\left(\frac{\sqrt{\Delta}}{b + 2cr_d}\right)\right.$$
$$\left.- \frac{2a + br_d}{\Delta(a + br_d + cr_d^2)}\right]_{R_1(\theta_d)}^{R_2(\theta_d)}\mathrm{d}\theta_d. \tag{17}$$

The variables Γ, a, b, c, and Δ have been defined in (15b)–(15f).

REFERENCES

[1] Y. C. Chow, A. R. Nix, and J. P. McGeehan, "Analysis of 16-APSK modulation in AWGN and Rayleigh fading channel," *Electron. Lett.*, vol. 28, pp. 1608–1610, Aug. 1992.

[2] F. Adachi and M. Sawahashi, "Performance analysis of various 16 level modulation schemes under Rayleigh fading," *IEEE Electron. Lett.*, vol. 28, pp. 1579–1581, Aug. 1992.

[3] Y. C. Chow, A. R. Nix, and J. P. McGeehan, "Diversity improvement for 16-DAPSK in Rayleigh fading channel," *IEEE Electron. Lett.*, vol. 29, pp. 387–389, Feb. 1993.

[4] Y. C. Chow, A. R. Nix, and J. P. McGeehan, "Error performance of circular 16-DAPSK with postdetection diversity reception in Rayleigh fading channels," *IEE Proc. Commun.*, vol. 144, pp. 180–190, June 1997.

[5] T. T. Tjhung, X. Dong, F. Adachi, and L. H. Tan, "On diversity reception of narrowband 16 star-QAM in fast Rician fading," *IEEE Trans. Veh. Technol.*, vol. 46, pp. 923–932, Nov. 1997.

[6] T. May, H. Rohling, and V. Engels, "Performance analysis of Viterbi decoding for 64-DAPSK and 64-QAM modulated OFDM signals," *IEEE Trans. Commun.*, vol. 46, pp. 182–190, Feb. 1998.

[7] J. Y. Lee, Y. M. Chung, and S. U. Lee, "Postdetection diversity receiver for DAPSK signals on the Rayleigh- and Rician-fading channel," *IEEE Trans. Veh. Technol.*, vol. 50, pp. 1193–1202, Sept. 2001.

[8] K. Liu, W. Wang, and Y. Liu, "High data rate transmission with 64-DAPSK over fading channel," in *Proc. IEEE WCNC*, Atlanta, GA, Mar. 2004.

[9] X. Dong and N. C. Beaulieu, "A new method for calculating symbol error probabilities of two-dimensional signalings in Rayleigh fading with channel estimation errors," *IEEE Trans. Commun.*, accepted for publication, available at http://www.ece.uvic.ca/~xdong/channel_err.pdf

[10] P. Gao and C. Tepedelenlioğli, "SNR estimation for nonconstant modulus constellations," *IEEE Trans. Signal Processing*, vol. 53, pp. 865–870, Mar. 2005.

[11] S. Benedetto and E. Biglieri, *Principles of Digital Transmission*, New York, NY: Kluwer Academic/Plenum Publishers, 1999.

[12] D. J. Young and N. C. Beaulieu, "The generation of correlated Rayleigh random variates by inverse discrete Fourier transform," *IEEE Trans. Commun.*, vol. 49, pp. 1114–1127, July 2000.

Lei Xiao received the B.Eng. degree in information engineering from the Teaching Reform Class (TRC), Shanghai Jiao Tong University, Shanghai, China in 2002, and the M.Sc. degree in Electrical and Computer Engineering from the University of Alberta, Edmonton, AB, Canada, in 2004. He is currently pursuing the Ph.D. degree in the Department of Electrical Engineering, University of Notre Dame, Notre Dame, IN, USA. His research interests include modulation, signal detection, and error control coding for wireless communications.

Xiaodai Dong received her B.Sc. degree in Information and Control Engineering from Xi'an Jiaotong University, China in 1992, her M.Sc. degree in Electrical Engineering from National University of Singapore in 1995 and her Ph.D. degree in Electrical and Computer Engineering from Queen's University, Kingston, ON, Canada in 2000.

She was with Nortel Networks, Ottawa, ON, Canada from 1999 to 2002, and involved in the base transceiver design of the third-generation (3G) mobile communication systems. From 2002 to 2004, she was an assistant professor at the Department of Electrical and Computer Engineering, University of Alberta, Edmonton, AB, Canada. She is presently an assistant professor and Canada research chair (Tier II) in ultra-wideband communications at the Department of Electrical and Computer Engineering, University of Victoria, Victoria, BC, Canada. Dr. Dong is an associate editor for IEEE Transactions on Communications and a member of IEEE. Her research interests include communication theory, modulation and coding, and ultra-wideband radio.
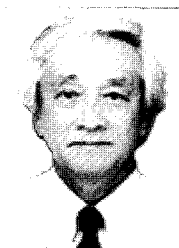
Tjeng Thiang Tjhung received the B.Eng. and M.Eng. Degrees in electrical engineering from Carleton University, Ottawa, Ontario, Canada, in 1963 and 1965, respectively, and the Ph.D. degree from Queen's University, Kingston, Ontario, Canada, in 1969.

From 1963 to 1968, he worked for Acres-Inter-Tel Ltd., Ottawa, as a consultant involved with the design of FSK systems for secure radio communication. In 1969, he joined the Department of Electrical Engineering, National University of Singapore, where he was appointed a professor in 1985. He retired from the University in March 2001, and joined the Institute for Infocomm Research in April 2001 as a principal scientist.

He was visiting scientist, from July to December 1991 at the Communication Research Centre in Ottawa Canada, and from January to March 1992 at the NTT Yokosuka Radio Communications Research Laboratories. He was visiting professor from March to May 1992 at Takushoku University, Tokyo, Japan and from May to July 1999 at the Broadband Wireless Laboratory, NTT Docomo, Yokosuka Research Laboratory. His present research interests are in, among others, multicarrier and code-division multiple-access (CDMA) techniques, space time coding and channel estimation in multiple input multiple output (MIMO) communication systems.

Dr. Tjhung is a senior member of the IEEE and a fellow of IES Singapore. He is also a member of the Association of Professional Engineers of Singapore.